Conditional Contact Angle Distribution in LEO Satellite-Relayed Transmission

Ruibo Wang, Anna Talgat, *Student Member, IEEE*, Mustafa A. Kishk, *Member, IEEE*,
and Mohamed-Slim Alouini, *Fellow, IEEE*

Abstract—This letter characterizes the contact angle distribution based on the condition that the relay low earth orbit (LEO) satellite is in the communication range of both the ground transmitter and the ground receiver. As one of the core distributions in stochastic geometry-based routing analysis, the analytical expression of the Cumulative Distribution Function (CDF) of the conditional contact angle is derived. Furthermore, the conditional contact angle is applied to analyze the inaccessibility of common satellites between the ground transmitter and receiver. Finally, with the help of the conditional contact angle, coverage probability and achievable data rate in LEO satellite-relayed transmission are studied.

Index Terms—Conditional contact angle distribution, stochastic geometry, satellite-relayed transmission, LEO satellite networks.

I. INTRODUCTION

IN RECENT years, the explosive growth of the number of LEO satellites has opened the door for many opportunities and challenges for the development of non-terrestrial networks [1], [2]. Because of the significant increase in the information-carrying capacity of the satellite network, more ground communications services can be transferred to space [3]. In the face of low latency and long-distance communication requirements, LEO satellites play an important role [4]. In a ground-satellite-ground transmission, the ground transmitter needs to associate with a reliable satellite as a relay. Compared with a high orbit satellite, one of the challenges a LEO satellite has to face is its relatively small coverage [5]. In addition, the interference from massive satellite constellations further decreases the communication region. Therefore, in addition to providing stronger power [6], the associated relay satellite should also locate within the reliable communication range of both the ground transmitter and receiver. The distribution of the distance between a strictly selected relay satellite and the ground transmitter is challenging but also meaningful. In relay transmission and routing problems [7], this distribution is the basis of many system parameter analyses [8].

Several related studies have appeared in recent years. They provide effective mathematical methods, accurate models, and practical methods for deriving the distance distribution [4], [9], [10]. Traditional deterministic network models that extend from cellular networks (such as the spherical Voronoi model) are not be suitable for large-scale dynamic network modeling. In addition to limiting the user's distance under single-hop communication, the spherical Voronoi model is not accurate to study the distance distribution [11]. Compared to the above modeling methods, the stochastic geometry-based method is undoubtedly more practical for irregular network modeling [12]. Among the existing stochastic geometry models, binomial point process (BPP) is relatively accurate for closed area networks with a fixed number of satellites [13], [14]. Some studies have given different forms of distance distribution between the ground receiver and the nearest satellite [6], [10], [14]. Since the satellites are distributed on the sphere, using angle to express the contact distance distribution is more concise. Therefore, contact angle distribution is introduced to analyze the coverage probability and latency of satellite networks [15], [16]. Based on the existing research, the contributions of this letter are summarized as follows.

- We derive an analytical expression of the contact angle distribution under the condition that the satellite is within the transmitter and receiver's communication range and its accuracy is verified.
- The influences of the number of satellites and the distance between the transmitter and receiver on the conditional contact angle are studied.
- Based on the conditional contact angle distribution, the satellite inaccessibility in single relay routing is analyzed and extended to multiple relays routing.
- We explain how to obtain coverage probability and achievable data rate of uplink from transmitter to relay satellite in routing by applying conditional contact angle.

II. SYSTEM MODEL

In this section, we build a ground-satellite-ground relay communication model. N_{Sat} satellites are distributed on a spherical surface with radius R_{Sat} and form a homogeneous BPP [14]. The transmitter and receiver are located on the Earth with distance d. The radius of the Earth is denoted as $R_{\oplus} = 6371 \text{km}$. We start with a simple scenario where a single satellite is selected as a relay, because the results obtained from a single satellite relay routing can be easily extended to a multiple one. A concrete example of the extension of satellite inaccessibility is provided in subsection IV-B.

We consider a satellite that maximizes the minimum quality of service of transmitter-satellite, and satellite-receiver links is suggested to be selected. Whether the data rate, coverage probability, or latency are negatively correlated with the communication distance, the quality of service can be measured

Fig. 1.   Satellite-relayed communication model.

Fig. 2.   Decomposition diagrams of the geometry combined by a cone and spherical cap.

by the reciprocal of the communication distance. However, when the relay satellites form a BPP, analysis of this strategy is intractable. Therefore, we consider a slightly suboptimal but tractable selection strategy: the transmitter is assumed to choose the closest satellite as a relay among the satellites that can provide reliable communication for both the transmitter and receiver [17].

Definition 1 (Dome Angle): Connect the two points with the center of the Earth, respectively, and the angle between the two connected lines is called the dome angle of two points.

Due to Earth blockage and maximum reliable communication distance, the transmitter and receiver can only communicate with satellites within a certain area. The certain area is a spherical cap which is the shaded area ($\mathcal{A}_1$ for transmitter, and $\mathcal{A}_2$ for receiver) in the top half of Fig. 1. The maximum dome angles of any two points in the spherical cap are denoted as $\theta_m^{(1)}$ and $\theta_m^{(2)}$, respectively, which are also called the maximum dome angles of two spherical caps $\mathcal{A}_1$ and $\mathcal{A}_2$. To ensure that $\mathcal{A}_1$ and $\mathcal{A}_2$ have intersecting region, the following equation should be satisfied

$$\theta_m^{(1)} + \theta_m^{(2)} > 4 \arcsin\left(\frac{d}{2R_\oplus}\right). \tag{1}$$

III. CONDITIONAL CONTACT ANGLE DISTRIBUTION

In this section, we derive the analytical expression of the CDF of the conditional contact angle distribution. The definition of the conditional contact angle is given below.

Definition 2 (Conditional Contact Angle): Among the satellites that can provide reliable communication for the receiver, the dome angle between the transmitter and its nearest satellite is called the conditional contact angle.

To derive the distribution of the conditional contact angle θ_c, the following steps are taken: (i) fixed the region $\mathcal{A}_2$ and dome angle $\theta_d^{(2)}$, continuously increase the dome angle $\theta_d^{(1)}$ of the spherical cap corresponding to the transmitter, (ii) calculate the intersecting area of the two spherical caps, and (iii) calculate the probability that there are no satellites in the intersection region.

To get the the intersecting area in step (ii), the irregular intersecting area can be divided into two parts by the red line, shown at the bottom of Fig. 1. These two parts correspond to
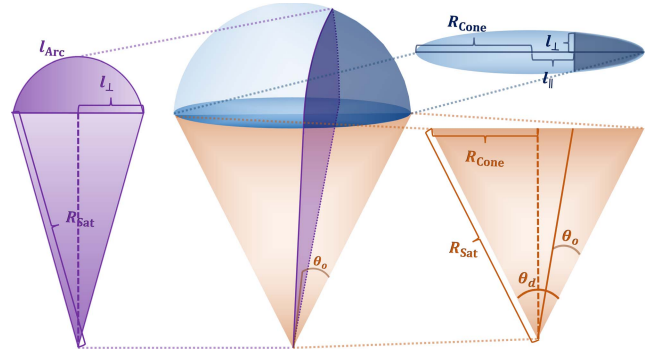
the right part of the left spherical cap and the left part of the right spherical cap. The following lemma can obtain the area of both regions. The two dome angles involved in the lemma are marked at the bottom of Fig. 1.

Lemma 1: For a spherical cap with dome angle θ_d, intercept the portion of one side of the cap, with dome angle θ_o. The area of the cut part $S(\theta_d, \theta_o)$ is given by,

$$S(\theta_d, \theta_o) = \int_{R_{\text{Sat}} \cos\frac{\theta_d}{2} \tan\left(\frac{\theta_d}{2} - \theta_o\right)}^{R_{\text{Sat}} \sin\left(\frac{\theta_d}{2}\right)} 2R_{\text{Sat}}$$
$$\times \arcsin\left(\frac{\sqrt{R_{\text{Sat}}^2 \sin\left(\frac{\theta_d}{2}\right)^2 - l^2}}{R_{\text{Sat}}}\right) dl. \tag{2}$$

Proof: See appendix A. □

Based on lemma 1, the CDF of the conditional contact distance is given in the following theorem.

Theorem 1: Given that the maximum dome angle of the receiver's spherical cap is $\theta_m^{(2)}$, the approximate CDF of the conditional contact angle $F_{\theta_c}(\theta)$ is given by,

$$F_{\theta_c}(\theta) = 1 - \left(1 - \frac{S\left(2\theta, \theta_o^{(1)}(\theta)\right) + S\left(\theta_m^{(2)}, \theta_o^{(2)}(\theta)\right)}{4\pi R_{\text{Sat}}^2}\right)^{N_{\text{Sat}}}, \tag{3}$$

where $\theta_o^{(1)}(\theta)$ and $\theta_o^{(2)}(\theta)$ are defined as,

$$\theta_o^{(1)}(\theta) = \theta - \frac{a(\theta)c - \sqrt{2a(\theta)^2 - 4a(\theta)b + 2b^2 + a(\theta)bc^2}}{a(\theta) - b},$$
$$\theta_o^{(2)}(\theta) = \frac{1}{2}\theta_m^{(2)} - \frac{-bc + \sqrt{2a(\theta)^2 - 4a(\theta)b + 2b^2 + a(\theta)bc^2}}{a(\theta) - b}, \tag{4}$$

where

$$a(\theta) = \cos\theta, \ b = \cos\frac{\theta_m^{(2)}}{2}, \ c = 2\arcsin\left(\frac{d}{2R_\oplus}\right), \tag{5}$$

and the domain of the contact angle is,

$$\max\left\{0, 2\arcsin\left(\frac{d}{2R_\oplus}\right) - \frac{1}{2}\theta_m^{(2)}\right\} \leq \theta_c$$
$$\leq \min\left\{\frac{1}{2}\theta_m^{(1)}, 2\arcsin\left(\frac{d}{2R_\oplus}\right) + \frac{1}{2}\theta_m^{(2)}\right\}. \tag{6}$$

Proof: See appendix B. □

IV. POTENTIAL APPLICATIONS

A. Satellite Inaccessibility in Single Relay Routing

One of the key issues in real-time and ultra long-distance routing is how far the distance between the transmitter and receiver can be or how many satellites are required to ensure that the routing will not be interrupted due to no available satellites. From theorem 1, an intuitive corollary about LEO relay outage probability can be obtained. The definition of LEO relay outage probability is given as follows.

Definition 3 (LEO Relay Outage Probability): The LEO relay outage probability is defined as the probability that there are no available satellites located in the communication range of both ground transmitter and receiver.

Corollary 1: Given that the Euclidean distance between the transmitter and receiver is d, the LEO relay outage probability $P_e^S(d)$ is given by,

$$P_e^S(d) = 1 - F_{\theta_c}\left(\min\left\{\frac{1}{2}\theta_m^{(1)}, 2\arcsin\left(\frac{d}{2R_\oplus}\right) + \frac{1}{2}\theta_m^{(2)}\right\}\right),$$

$$(7)$$

where the CDF of the conditional contact angle $F_{\theta_c}(\theta)$ is defined in (3).

B. Satellite Inaccessibility in Multiple Relays Routing

With the above corollary, designers can keep the outage probability below a threshold by adjusting d and N_{Sat}. However, only studying the satellite inaccessibility in single satellite relay routing is quite limited. The transmitter requires multiple relay satellites to send the message to the receiver in most cases. Therefore, we consider the satellite inaccessibility in a routing consisting of multiple satellite relays with a bent pipe architecture [18].

In such an architecture, $N_h - 1$ terrestrial relays are required when N_h relay satellites are selected. In order to reduce latency and power consumption, we assume that every two adjacent terrestrial relays have the same dome angle. Therefore, the multiple relays outage probability $P_e^M(N_h, d)$, which is the probability that there are no satellites available in any hop, is given in the following corollary. Since $P_e^M(N_h, d)$ can be derived from $P_e^S(d)$ by simple geometric relations, the proof is omit here.

Corollary 2: Given that the Euclidean distance between the transmitter and receiver is d, the multiple relays outage probability $P_e^M(d)$ is expressed as,

$$P_e^M(N_h, d)$$
$$= 1 - \left(1 - P_e^S\left(2R_\oplus\sin\left(\frac{1}{N_h}\arcsin\left(\frac{d}{2R_\oplus}\right)\right)\right)\right)^{N_h}, \quad (8)$$

where $P_e^S(d)$ is defined in (7) and N_h is the number of selected relay satellites.

The N_h needs to be carefully designed according to the multiple relays outage probability. Generally speaking, a long-hop strategy (with a small N_h) leads to a larger outage probability, while a short-hop strategy (with a large N_h) leads to a larger latency [16].
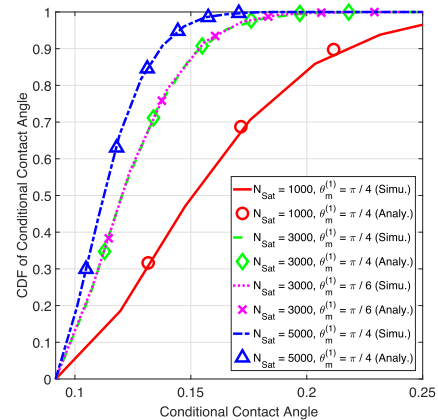

Fig. 3. CDF of the conditional contact angle under different number of satellites and the maximum dome angle of the transmitter.

C. Uplink Coverage and Rate Analysis With Suboptimal Relay Selection

Coverage probability and achievable maximum data rate are highlighted metrics of satellite network analysis. In the case of satellites providing coverage to ground users, the authors in [13] and [14] provide analytical expressions of downlink coverage probability and achievable data rate, respectively. The above expressions can be modified into uplink coverage probability and achievable data rate from transmitter to satellite in the routing scenario. The modification process is straightforward, and the only task is replacing the contact distance with the conditional contact distance. Notice that the domain of contact distance also needs to be replaced. Conditional contact distance is defined as the distance from the transmitter to the closest satellite that can provide reliable communication for both the transmitter and receiver. The relationship between the conditional contact distance d_c and conditional contact angle θ_c is,

$$2\,R_\oplus R_{\text{Sat}}\cos\theta_c = R_\oplus^2 + R_{\text{Sat}}^2 - d_c^2. \quad (9)$$

V. NUMERICAL RESULTS

In this section, numerical results of the CDF of the conditional contact angle are provided. As shown in Fig. 3 and Fig. 4, the analytical results perfectly match the simulation results, which proves the accuracy of theorem 3. The height of satellites is fixed at 550km and $R_{\text{Sat}} = 6921$km. The maximum dome angle of the receiver is $\theta_m^{(2)} = \frac{\pi}{4}$.

In Fig. 3, the distributions of the conditional contact angle under the different number of satellites N_{Sat} and the maximum dome angle of the transmitter $\theta_m^{(1)}$ are studied. The distance between the ground transmitter and receiver is fixed as $d = 3000$km. Reducing N_{Sat} causes the CDF curve to move down. Changing $\theta_m^{(1)}$ does not have significant effects on the CDF.

Fig. 4 describes the influence of the distance between the transmitter and receiver on the distribution of the conditional contact angle. The number of satellites is fixed as $N_{\text{Sat}} = 3000$, and the maximum dome angle of the transmitter is $\theta_m^{(1)} = \frac{\pi}{4}$. As the distance between the transmitter and receiver decreases, the CDF curve is shifted from right to left, with little change in shape. Finally, the conditional contact
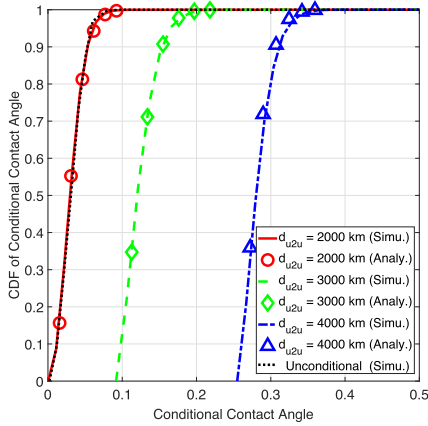
Fig. 4. CDF of the conditional contact angle under different distance between the transmitter and receiver.
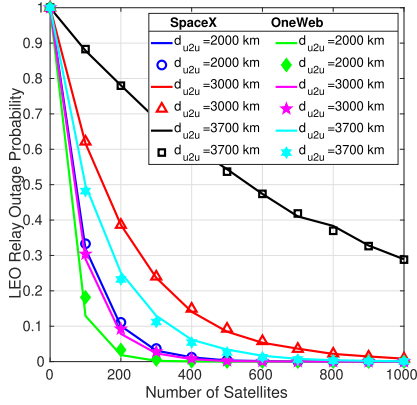

Fig. 5. LEO relay outage probability under different distance between the transmitter and receiver and constellation altitudes.

angle distribution converges to the unconditional contact angle distribution.

In Fig. 5, the LEO relay outage probability, $P_e^S(d)$, is studied under different values for the distance between the transmitter and receiver for companies OneWeb and SpaceX with altitudes $h = 1200$km and $h = 550$km, respectively. The outage probability gets larger as we increase the distance between the transmitter and receiver. We observe that for the larger altitude of OneWeb, we have less LEO relay outage probability compared with SpaceX for each distance.

VI. Conclusion

In this letter, we derived the approximate conditional contact angle distribution based on the stochastic geometry framework. Three Potential applications of conditional contact angles are further given. Finally, we provide the numerical results about the influence of the number of satellites, the distance between the transmitter and receiver on the conditional contact angle. For the lower altitude of the satellite constellation, it is better to keep the distance less than 3000km to ensure that there are available satellites between the transmitter and receiver for a single-hop transmission.

APPENDIX A
PROOF OF LEMMA 1

As shown in Fig. 2, the middle part is a geometry composed of a spherical cap and a cone. The right (dark blue) part of the

spherical cap in the geometry corresponds to the dome angle θ_o. According to the description in the lemma, the area of the dark blue part is the desired $S(\theta_d, \theta_o)$. Divide the dome angle θ_o into infinitesimal $\Delta\theta_o$. The dark blue area can be divided into numerous arcs. $S(\theta_d, \theta_o)$ is calculated by multiplying the sum of these arcs by $\Delta\theta_o$. Project the spherical cap on the circle in the upper right corner of Fig. 2. The relationship between the arc length l_{Arc} and the chord length obtained by projection is given by,

$$l_{\text{Arc}} = 2R_{\text{Sat}} \arcsin \frac{l_\perp}{R_{\text{Sat}}}, \qquad (10)$$

where $l_\perp$ is half of the chord length. Since there is a one-to-one mapping between chord length and arc length, $S(\theta_d, \theta_o)$ can be obtained by integrating the region on the right side of the circle. As shown in the upper right part of Fig. 2, we choose to integrate in the direction perpendicular to the chord. Easy to know that

$$R_{\text{Cone}}^2 = l_{//}^2 + l_\perp^2 = R_{\text{Sat}} \sin\left(\frac{\theta_d}{2}\right). \qquad (11)$$

where R_{Cone} is the radius of the projected circle. Set the center of the circle as the origin. The upper bound of the integral is R_{Cone}, and the lower bound is given by,

$$\tan\left(\frac{\theta_d}{2} - \theta_o\right) = \frac{l_{//}^{\text{low}}}{R_{\text{Sat}} \cos\frac{\theta_d}{2}}. \qquad (12)$$

The integral of $S(\theta_d, \theta_o)$ is calculated as follows,

$$\begin{aligned}
S(\theta_d, \theta_o) &= \int_{l_{//}^{\text{low}}}^{R_{\text{Cone}}} l_{\text{Arc}}(l)\, \mathrm{d}l \\
&= \int_{l_{//}^{\text{low}}}^{R_{\text{Cone}}} 2R_{\text{Sat}} \arcsin\left(\frac{l_\perp}{R_{\text{Sat}}}\right) \mathrm{d}l \\
&= \int_{l_{//}^{\text{low}}}^{R_{\text{Cone}}} 2R_{\text{Sat}} \arcsin\left(\frac{\sqrt{R_{\text{Cone}}^2 - l^2}}{R_{\text{Sat}}}\right) \mathrm{d}l.
\end{aligned} \qquad (13)$$

Substitute (11) and (12) into (13), the final result of the lemma is obtained. In addition, $l_{//}^{\text{low}}$ might be less than 0. It's guaranteed that the lower bound of the integral is always less than the upper bound because,

$$\cos\frac{\theta_d}{2} \tan\left(\frac{\theta_d}{2} - \theta_o\right) < \cos\frac{\theta_d}{2} \tan\left(\frac{\theta_d}{2}\right) = \sin\left(\frac{\theta_d}{2}\right). \qquad (14)$$

APPENDIX B
PROOF OF THEOREM 1

By definition, the CDF of the conditional contact angle can be expressed as,

$$\begin{aligned}
F_{\theta_c}(\theta) &= 1 - \mathbb{P}[\theta_c > \theta] = 1 - \mathbb{P}[\mathcal{N}(\mathcal{A}_o) = 0] \\
&\overset{(a)}{=} 1 - \left(1 - \frac{S\left(\frac{1}{2}\theta_d^{(1)}, \theta_o^{(1)}\right) + S\left(\frac{1}{2}\theta_d^{(2)}, \theta_o^{(2)}\right)}{4\pi r^2}\right)^{N_{\text{Sat}}},
\end{aligned} \qquad (15)$$

where $\mathcal{N}(\mathcal{A}_o)$ counts the number of the satellites in the overlap region $\mathcal{A}_o$. For a homogeneous BPP, the probability

of the satellite locates in $\mathcal{A}_o$ is equal to the ratio of the area of $\mathcal{A}_o$ to the total surface area of the sphere. As shown in the bottom of Fig. 1, $\mathcal{A}_o$ is divided into two parts, with dome angles $\theta_o^{(1)}$ and $\theta_o^{(2)}$. In step (a), the area of $\mathcal{A}_o$ is equal to the sum of $S\left(\frac{1}{2}\theta_d^{(1)}, \theta_o^{(1)}\right)$ and $S\left(\frac{1}{2}\theta_d^{(2)}, \theta_o^{(2)}\right)$, which are defined in (2).

When dome angles $\theta_o^{(1)}$, $\theta_o^{(2)}$ and the distance between the transmitter and receiver d are given, $\theta_o^{(1)}$ and $\theta_o^{(2)}$ can be represented by them. From the relationship between these dome angles,

$$\frac{\theta_d^{(1)}}{2} + \frac{\theta_d^{(2)}}{2} - \theta_o^{(1)} - \theta_o^{(2)} = 2\arcsin\left(\frac{d}{2R_\oplus}\right). \quad (16)$$

Since two right triangles share the red cutting line, the following equation can be obtained,

$$\frac{R_{\text{Sat}}\cos\left(\frac{1}{2}\theta_d^{(1)}\right)}{\cos\left(\frac{1}{2}\theta_d^{(1)} - \theta_o^{(1)}\right)} = \frac{R_{\text{Sat}}\cos\left(\frac{1}{2}\theta_d^{(2)}\right)}{\cos\left(\frac{1}{2}\theta_d^{(2)} - \theta_o^{(2)}\right)} \quad (17)$$

Combine (16) and (17), $\theta_o^{(1)}$ and $\theta_o^{(2)}$ can be derived theoretically. However, it isn't easy to obtain an analytical solution for the two dome angles for this system of trigonometric equations. So we approximate the cosine function by a second-order Taylor expansion,

$$\cos\left(\frac{\theta_d}{2} - \theta_o\right) \approx 1 - \left(\frac{1}{2}\theta_d - \theta_o\right)^2, \quad (18)$$

Substitute (18) into (17), we get

$$\frac{\cos\left(\frac{1}{2}\theta_d^{(1)}\right)}{1 - \left(\frac{1}{2}\theta_d^{(1)} - \theta_o^{(1)}\right)^2} = \frac{\cos\left(\frac{1}{2}\theta_d^{(2)}\right)}{1 - \left(\frac{1}{2}\theta_d^{(2)} - \theta_o^{(2)}\right)^2}. \quad (19)$$

Combine (16) and (19), the approximate solution is expressed as,

$$\theta_o^{(1)}\left(\theta_d^{(1)}\right) \approx \frac{1}{2}\theta_d^{(1)} - \frac{ac - \sqrt{2a^2 - 4ab + 2b^2 + abc^2}}{a - b},$$
$$\theta_o^{(2)}\left(\theta_d^{(2)}\right) \approx \frac{1}{2}\theta_d^{(2)} - \frac{-bc + \sqrt{2a^2 - 4ab + 2b^2 + abc^2}}{a - b},$$
$$(20)$$

where a, b and c are defined as follows,

$$a = \cos\left(\frac{1}{2}\theta_d^{(1)}\right), \quad b = \cos\left(\frac{1}{2}\theta_d^{(2)}\right), \quad c = 2\arcsin\left(\frac{d}{2R_\oplus}\right). \quad (21)$$

In this case, $\theta_d^{(2)}$ is fixed as a constant $\theta_m^{(2)}$, while $\theta_d^{(1)}$ is twice the conditional contact angle θ_c. In formula (15), substitute $\theta_m^{(2)}$ into $\theta_d^{(2)}$ and $2\theta_c$ into $\theta_d^{(1)}$ to get the final result.

The remaining problem is to determine the range of θ_c. The relay satellite must be within the reliable communication range of the transmitter, so $0 \leq \theta_c \leq \theta_m^{(1)}$ is required. To ensure that the two caps intersect,

$$2\theta_c + \theta_m^{(2)} \geq 4\arcsin\left(\frac{d}{2R_\oplus}\right). \quad (22)$$

However, when θ_c is too large, the transmitter's cap may contain the receiver's cap, and increasing θ_c further is meaningless. Therefore, we have,

$$2\theta_c \leq 4\arcsin\left(\frac{d}{2R_\oplus}\right) + \theta_m^{(2)}. \quad (23)$$

In addition, to ensure that the relay satellite is always within the receiver's line of sight, the following inequalities always need to be satisfied,

$$\theta_m^{(i)} < 2\arcsin\frac{d}{2R_\oplus}, \quad i = 1, 2. \quad (24)$$

REFERENCES

[1] O. Kodheli *et al.*, "Satellite communications in the new space era: A survey and future challenges," *IEEE Commun. Surveys Tuts.*, vol. 23, no. 1, pp. 70–109, 1st Quart., 2021.

[2] S. C. Ekpo, B. Adebisi, D. George, R. Kharel, and M. Uko, "System-level multicriteria modelling of payload operational times for communication satellite missions in LEO," *Recent Prog. Space Technol.*, vol. 4, no. 1, pp. 67–77, Jun. 2014.

[3] N. Saeed, A. Elzanaty, H. Almorad, H. Dahrouj, T. Y. Al-Naffouri, and M.-S. Alouini, "CubeSat communications: Recent advances and future challenges," *IEEE Commun. Surveys Tuts.*, vol. 22, no. 3, pp. 1839–1862, 3rd Quart., 2020.

[4] R. Wang, M. A. Kishk, and M.-S. Alouini, "Ultra-dense LEO satellite-based communication systems: A novel modeling technique," *IEEE Commun. Mag.*, vol. 60, no. 4, pp. 25–31, Apr. 2022.

[5] F. Vatalaro, G. E. Corazza, C. Caini, and C. Ferrarelli, "Analysis of LEO, MEO, and GEO global mobile satellite systems in the presence of interference and fading," *IEEE J. Sel. Areas Commun.*, vol. 13, no. 2, pp. 291–300, Feb. 1995.

[6] N. Okati and T. Riihonen, "Nonhomogeneous stochastic geometry analysis of massive LEO communication constellations," *IEEE Trans. Commun.*, vol. 70, no. 3, pp. 1848–1860, Mar. 2022.

[7] M. Haenggi, "On routing in random Rayleigh fading networks," *IEEE Trans. Wireless Commun.*, vol. 4, no. 4, pp. 1553–1562, Jul. 2005.

[8] J. G. Andrews, A. K. Gupta, and H. S. Dhillon, "A primer on cellular network analysis using stochastic geometry," 2016, *arXiv:1604.03183*.

[9] A. Al-Hourani, "Session duration between handovers in dense LEO satellite networks," *IEEE Wireless Commun. Lett.*, vol. 10, no. 12, pp. 2810–2814, Dec. 2021.

[10] A. Talgat, M. A. Kishk, and M.-S. Alouini, "Nearest neighbor and contact distance distribution for binomial point process on spherical surfaces," *IEEE Commun. Lett.*, vol. 24, no. 12, pp. 2659–2663, Dec. 2020.

[11] A. Kak and I. F. Akyildiz, "Large-scale constellation design for the Internet of Space Things/CubeSats," in *Proc. IEEE Globecom Workshops (GC Wkshps)*, Dec. 2019, pp. 1–6.

[12] M. Haenggi, *Stochastic Geometry for Wireless Networks*. Cambridge, U.K.: Cambridge Univ. Press, 2012.

[13] A. Talgat, M. A. Kishk, and M.-S. Alouini, "Stochastic geometry-based analysis of LEO satellite communication systems," *IEEE Commun. Lett.*, vol. 25, no. 8, pp. 2458–2462, Aug. 2021.

[14] N. Okati, T. Riihonen, D. Korpi, I. Angervuori, and R. Wichman, "Downlink coverage and rate analysis of low Earth orbit satellite constellations using stochastic geometry," *IEEE Trans. Commun.*, vol. 68, no. 8, pp. 5120–5134, Aug. 2020.

[15] A. Al-Hourani, "An analytic approach for modeling the coverage performance of dense satellite networks," *IEEE Wireless Commun. Lett.*, vol. 10, no. 4, pp. 897–901, Apr. 2021.

[16] R. Wang, M. A. Kishk, and M.-S. Alouini, "Stochastic geometry-based low latency routing in massive LEO satellite networks," 2022, *arXiv:2204.03802*.

[17] K. Belbase, Z. Zhang, H. Jiang, and C. Tellambura, "Coverage analysis of millimeter wave decode-and-forward networks with best relay selection," *IEEE Access*, vol. 6, pp. 22670–22683, 2018.

[18] A. Gaber, M. A. ElBahaay, A. M. Mohamed, M. M. Zaki, A. S. Abdo, and N. AbdelBaki, "5G and satellite network convergence: Survey for opportunities, challenges and enabler technologies," in *Proc. 2nd Novel Intell. Lead. Emerg. Sci. Conf. (NILES)*, Oct. 2020, pp. 366–373.